# Inorganic Chemistry

Calorimetric Investigation of Copper Binding in the N-Terminal Region of the Prion Protein at Low Copper Loading: Evidence for an Entropically Favorable First Binding Event

Devi Praneetha Gogineni, Anne M. Spuches, and Colin S. Burns*

Department of Chemistry, East Carolina University, East 5th Street, Greenville, North Carolina 27858, United States

S *Supporting Information*

ABSTRACT: Although the Cu^{2+}-binding sites of the prion protein have been well studied when the protein is fully saturated by Cu^{2+}, the Cu^{2+}-loading mechanism is just beginning to come into view. Because the Cu^{2+}-binding modes at low and intermediate Cu^{2+} occupancy necessarily represent the highest-affinity binding modes, these are very likely populated under physiological conditions, and it is thus essential to characterize them in order to understand better the biological function of copper−prion interactions. Besides binding-affinity data, almost no other thermodynamic parameters (e.g., ΔH and ΔS) have been measured, thus leaving undetermined the enthalpic and entropic factors that govern the free energy of Cu^{2+} binding to the prion protein. In this study, isothermal titration calorimetry (ITC) was used to quantify the thermodynamic parameters (K, ΔG, ΔH, and $T\Delta S$) of Cu^{2+} binding to a peptide, PrP(23−28, 57−98), that encompasses the majority of the residues implicated in Cu^{2+} binding by full-length PrP. Use of the buffer N-(2-acetomido)-amino-ethanesulfonic acid (ACES), which is also a well-characterized Cu^{2+} chelator, allowed for the isolation of the two highest affinity binding events. Circular dichroism spectroscopy was used to characterize the different binding modes as a function of added Cu^{2+}. The K_d values determined by ITC, 7 and 380 nM, are well in line with those reported by others. The first binding event benefits significantly from a positive entropy, whereas the second binding event is enthalpically driven. The thermodynamic values associated with Cu^{2+} binding by the Aβ peptide, which is implicated in Alzheimer's disease, bear striking parallels to those found here for the prion protein.
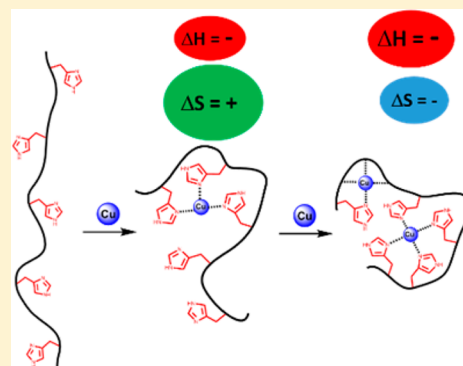
INTRODUCTION

The normal cellular form of the prion protein (PrP^C) is tethered to the outer surface of neuronal cells through a glycosylphosphatidylinositol (GPI) anchor.[1] PrP^C undergoes endocytosis where it cycles between the endosome and cell surface,[2] and this is dramatically stimulated by exposure to divalent copper and, to a lesser extent, zinc.[3] The observation that PrP binds Cu^{2+} in vivo and the fact that the N-terminal metal-binding region is highly conserved in mammals strongly suggests the PrP−Cu^{2+} interaction plays a physiological role.[4,5] The specific interaction of PrP with Cu^{2+} serves as a lens through which the normal function, and possibly the disease causing refolding of PrP^C to the *scrapie* form (PrP^{Sc}), can be studied.

At physiological pH, PrP binds approximately 5 equiv of Cu^{2+} ions at the unstructured N-terminal half of the protein, residues 60−111.[4,6−9] The octarepeat region, residues 60−91, binds 4 equiv of Cu^{2+} and consists of four sequential repeats of PHGGGWGQ.[10−12] Immediately following the octarepeats is a region spanning residues 92−111 that contains two His residues (His96 and His111) and is involved in the binding of 1 equiv of Cu^{2+}.[13−15] Although the structure of the Cu^{2+}-coordination sphere for the octarepeat region is well established in its fully Cu^{2+}-saturated state, the precise Cu^{2+}-coordination sphere of the C-terminal site (the so-called "fifth" or "non-octarepeat" site) is not as well resolved.

The Cu^{2+}-loading mechanism of the metal-binding domain of PrP is complex, involving three different binding modes, some of which are composed of multiple isomers, and depends on the precise ratio of Cu^{2+} to PrP.[16−18] There is consensus that the initial binding event involves coordination of Cu^{2+} by multiple His imidazoles, most of which are located in the octarepeat region. However, the question as to which His residues are involved differs between studies because different model peptides have been used, many of which have less than the six His residues contained in the region of PrP that spans residues 60−111. The second binding event occurs at the nonoctarepeat site, and any further addition of Cu^{2+} begins to populate the individual octarepeat units (HGGGW−Cu^{2+}) at the expense of the multiple-His binding mode.[18−20]

Extracellular Cu^{2+} concentrations in the central nervous system (CNS) are estimated to be in the low micromolar range,[21−23] and PrP has K_d values ranging from subnanomolar to

Table 1. PrP-Derived Peptide Sequences[a]

Peptide	Sequence
PrP(23-28, 57-98)	KKRPKP WGQPHGGGWGQWPHGGGWGQWPHGGGWGQWPHGGGWGQGGGTHNQ
PrP(89-98)	WGQGGGTHNQ
PrP(84-91)	PHGGGWGQ

[a]All of the peptides were acetylated at the N-terminus and amidated at the C-terminus.

low micromolar.[7−9,17,24] Thus, PrP is tuned for binding in this environment and is responsive to a wide range of copper concentrations. Deeper insight into the highest-affinity binding modes, both structurally and thermodynamically, would be beneficial because they are very likely populated under physiological conditions where the Cu^{2+} concentration is low and/or there are competitors. Although a number of spectroscopic and spectrometric studies have provided some structural information about the high-affinity sites, almost no thermodynamic information is available. A few studies using isothermal titration calorimetry (ITC) on the binding of Cu^{2+} by PrP have been performed from which stoichiometries and K_d values have been determined.[8,19,25] However, other thermodynamic parameters, such as ΔG, ΔH, and ΔS, have not been measured, thus leaving the enthalpic and entropic factors governing the free energy of binding undetermined.

In this Article, ITC was used to quantify the thermodynamic parameters for Cu^{2+} binding to PrP(23−28, 57−98) and circular dichroism (CD) spectroscopy was used to characterize the different binding modes as a function of added Cu^{2+}. This particular peptide construct was utilized because it encompasses the majority of the residues implicated in Cu^{2+} binding by full-length PrP, and its Cu^{2+}-loading process as well as its Cu^{2+}-coordination spheres have already been well characterized by our lab.[18,20] The K_d values determined by ITC are well in line with those reported by others.[17,24] Interestingly, the enthalpy associated with the second binding event ($\Delta H_2 = -37.2 \pm 5\%$ kcal/mol) is significantly higher than that of the first binding event ($\Delta H_1 = -3.59 \pm 13\%$ kcal/mol). However, the entropy for the first binding event is positive ($T\Delta S_1 = +2.18 \pm 23\%$ kcal/mol), which helps to offset the enthalpy difference and leads to a K_d that is 2 orders of magnitude smaller (i.e., higher affinity). The thermodynamic values associated with Cu^{2+} binding by the Aβ peptide,[26] implicated in Alzheimer's disease, bear striking parallels to those found here for PrP. Thus, a favorable entropy associated with initial metal binding may be a general property of highly flexible systems such as PrP and Aβ where equilibria between coordination spheres exists and multiple histidine residues are present.

EXPERIMENTAL METHODS

Peptide Synthesis. All peptides were prepared by solid-phase synthesis on an automated PS3 synthesizer (Protein Technologies, Inc.) using standard fluorenylmethoxycarbonyl (Fmoc) methods, purified by reverse-phase HPLC (C18 column), and characterized by electrospray ionization mass spectrometry on a Micromass Q-ToF micro (Agilent). The three peptides used for this study are shown in Table 1. All of the peptides were acetylated at the N-terminus and amidated at the C-terminus.

Peptide Sample Preparation and Concentration Determination. Lyophilized peptides were dissolved in buffer containing 10 mM N-(2-acetamido)-2-aminoethanesulfonic acid (ACES) at pH 7.4 or 10 mM N-ethylmorpholine (NEM) at pH 7.4. Peptide concentrations were determined by acquiring UV−vis spectra of the samples. The extinction coefficient for tryptophan at 280 nm, which was taken as 5690

M^{-1} cm^{-1}, was used to calculate the peptide concentration. Copper (Cu^{2+}) was added as $CuCl_2$.

Circular Dichroism Spectroscopy. CD spectra were collected at room temperature on a J-815 spectrometer (Jasco) with a bandwidth of 4 nm in a 1 cm cell. To ensure accurate background subtraction for each sample, a background spectrum of the buffer was collected immediately after every run. The PMT high voltage was below 400 V in the range of 290 nm 680 nm. As recommended by Jasco, 400 V was selected as the threshold beyond which data may be considered excessively noisy and thus unreliable.

Isothermal Titration Calorimetry. ITC measurements were carried out at 25 °C on a MicroCal VP-ITC ultrasensitive titration calorimeter. The solution in the cell was stirred at 307 rpm to ensure rapid mixing. In each experiment, 8 μL of titrant was delivered to the reaction cell over 20 s with a 350 s interval between injections to allow complete equilibration. Titrations were run in triplicate for each peptide to ensure reproducibility and to allow for statistical analysis. A background titration consisting of the identical titrant solution but containing only the buffer solution in the sample cell was run for each reaction (Figure S1). The last ten data points were averaged and subtracted from each experimental titration to account for the heat of dilution. The data were subsequently analyzed with a sequential binding model included in the Origin 7.0 software package supplied by MicroCal.

RESULTS

ACES was used as a buffer and as the chelator for Cu^{2+}. To determine how effective it was at preventing Cu^{2+} loading of the octarepeat units, visible CD spectroscopy was utilized to characterize the different binding modes as a function of added Cu^{2+}. The absorption bands that are due to d−d transitions can occur over a range of wavelengths, typically 500−750 nm. In CD spectroscopy, the transitions for Cu^{2+} typically arise in pairs: one being a positive band and the other a negative band. CD spectroscopy has the advantage of being able to resolve transitions that overlap in regular absorbance spectra, and these appear as separate bands. The technique is very sensitive to the metal−ligand sphere, and this is reflected by both the absorbance extrema and the phase associated with the transition (i.e., positive or negative).[27] Furthermore, these transitions become observable by CD spectroscopy only when Cu^{2+} is in a chiral ligand environment; unbound aqueous Cu^{2+} is not detected. The CD spectroscopy signals characteristic of the two different coordination spheres populated when PrP(23−28, 57−98) is fully Cu^{2+}-saturated (i.e., HGGGW−Cu^{2+} and GTH−Cu^{2+}) have been described previously.[10,11,14,17,20,28] Figure 1a shows the CD spectrum of PrP(23−28, 57−98) with 5 equiv of Cu^{2+} in 10 mM ACES. (See Table 1 for peptide sequences.)

At this point in the process, the system is considered to be saturated with Cu^{2+} because further addition of the metal (up to 10 equiv of Cu^{2+}) results in no change in the CD signal (data not shown). It should be noted that the highest-affinity binding mode (i.e., that of multiple His residues coordinating a single Cu^{2+}) is CD silent. The CD signal observed in Figure 1a closely resembles that of the GTH−Cu^{2+} complex (Figure 1b) modeled by PrP(89−98), with the λ_{max} (∼500 nm) values of the positive bands being almost identical. Here, we focus mainly on the
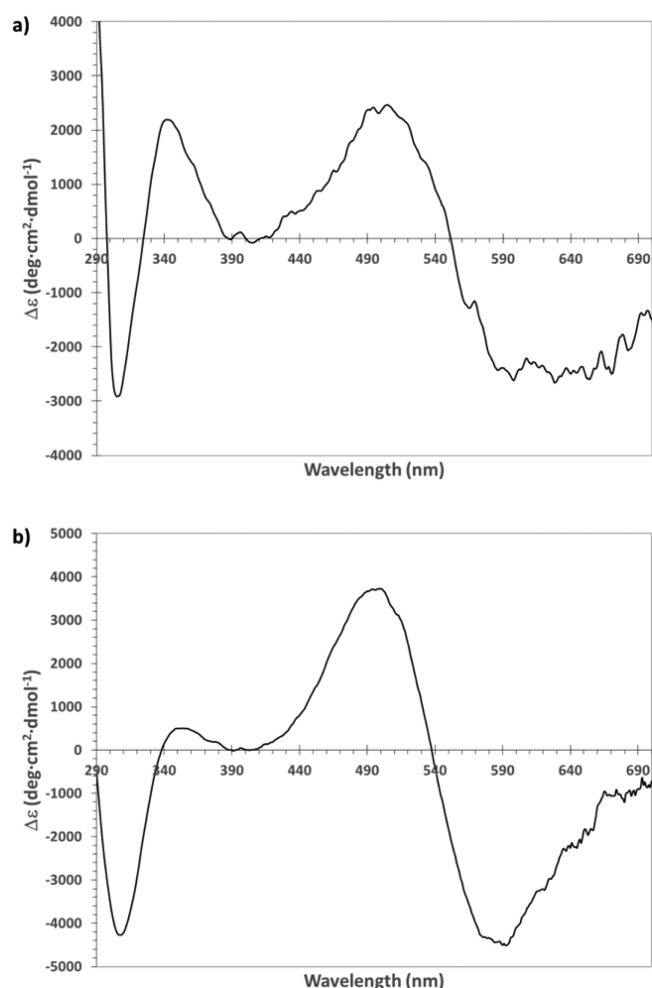
Figure 1. (a) Visible CD spectrum of 0.1 mM PrP(23−28, 57−98) with 0.5 mM Cu^{2+} added in 10 mM ACES, pH 7.4. (b) Visible CD spectrum of 0.2 mM PrP(89−98)/Cu^{2+} in 10 mM NEM, pH 7.4.

positive band at 500 nm because the negative band (λ_{min}), which appears at wavelengths greater than 580 nm, suffers from excessive noise for PrP(23−28, 57−98) (Figure 1a). Above 625 nm, the photomultiplier tube (PMT) high voltage began to exceed 400 V, which is considered by the instrument manufacturer to be the threshold beyond which data may be considered excessively noisy and thus unreliable. However, the negative differential absorbances in Figure 1a,b are not dissimilar because they both appear in the 580−690 nm range. The additional absorption band, centered at approximately 330 nm with a positive band near 350 nm and a negative band near 310 nm, is attributable to the ligand-to-metal charge transfer (LMCT) band arising from the excitation of electrons from the imidazole group and/or deprotonated amide(s) to the copper center. These bands are not as informative or as well-correlated to particular equatorial ligand arrangements for PrP−Cu^{2+} complexes as those arising from d−d transitions.[20,29] Herein, we note that the intensities of the LMCT bands are different and may reflect slight distortions in the equatorial coordination sphere as a result of different peptide models being used.

Thus, the data suggests that the PrP(23−28, 57−98) peptide binds two Cu^{2+} ions and the octarepeat units (i.e., the four HGGGW segments) fail to out-compete the ACES buffer for Cu^{2+}. To corroborate this conclusion, the visible CD spectrum of

PrP(73−91) in complex with Cu^{2+} was collected in the absence (Figure 2) and presence of ACES. Upon the addition of ACES, the CD signal disappeared (data not shown).
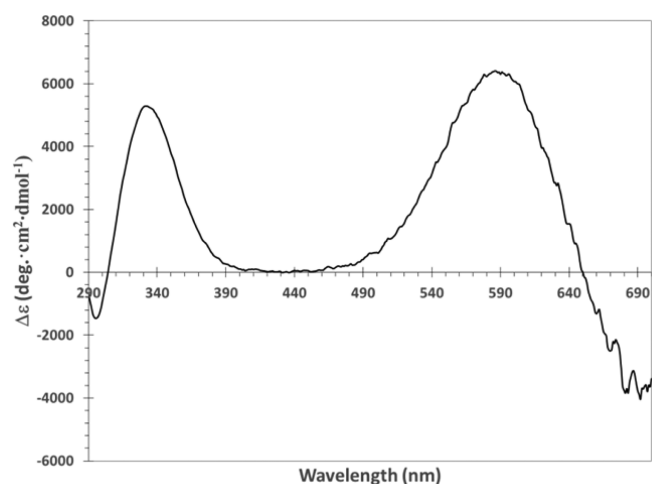

Figure 2. Visible CD spectrum of 0.2 mM PrP(73−91)/Cu^{2+} in 10 mM NEM, pH 7.4.

ITC was used to measure the heat associated with the titration of Cu^{2+} into PrP(23−28, 57−98) in 10 mM ACES buffer, pH 7.4 at 298 K. Three separate ITC experiments were performed under identical conditions. A representative titration is shown in Figure 3, displaying the differential power signal measured for each
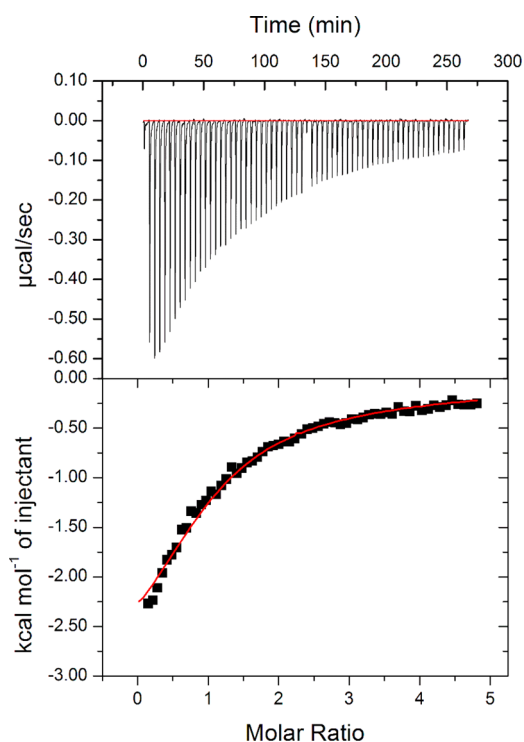

Figure 3. ITC binding isotherm for the titration of Cu^{2+} into 0.1 mM PrP(23−28, 57−98) in 10 mM ACES, pH 7.4 at 25 °C. The top panel shows the differential power signal measured for each injection, and the bottom panel shows the integrated peak areas corresponding to the measured heat released for each injection. A theoretical fit is superimposed on the data and the resulting thermodynamic parameters are listed in Table S1 (Run 1).
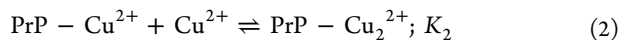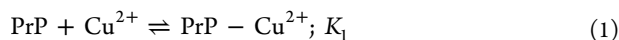
injection and isotherm (top and bottom, respectively). The binding isotherm shows saturation behavior with no clear inflection point. This suggests that the Cu^{2+}/PrP ratio is greater than 1:1 (i.e., there is more than one Cu^{2+} bound per peptide). Buffer- and pH-dependent binding constants and thermodynamic values were obtained by fitting of the binding isotherm (Table 2).

Table 2. Best-Fit Isothermal Titration Calorimetry Parameters and Buffer-Dependent Thermodynamic Values for PrP(23−28, 57−98)[a]

thermodynamic parameters	average values (%, $n = 3$)
K_1[b]	1.71 ± 12
K_2[c]	154 ± 28
ΔH_1[d]	-3.59 ± 13
ΔH_2[d]	-37.2 ± 5
$T\Delta S_1$[d]	2.18 ± 23
$T\Delta S_2$[d]	-34.3 ± 55

[a]The values shown are the average of fits from three runs (Figures S2, S3, and S4), and error is reported as ±1 standard deviation in percent. [b]Represented in (moles per liter)$^{-1} \times 10^4$. [c]Represented in (moles per liter)$^{-1}$. [d]Represented in kilocalories per mole.

A sequential binding model with two sites (i.e., $Cu^{2+}/PrP = 2:1$) provides the best fit and is congruent with the stoichiometry suggested by the CD spectroscopy data, represented as

$$PrP + Cu^{2+} \rightleftharpoons PrP - Cu^{2+}; \quad K_1 \tag{1}$$

$$PrP - Cu^{2+} + Cu^{2+} \rightleftharpoons PrP - Cu_2^{2+}; \quad K_2 \tag{2}$$

where K_1 and K_2 are defined as

$$K_1 = \frac{[PrP - Cu^{2+}]}{[PrP][Cu^{2+}]} \tag{3}$$

$$K_2 = \frac{[PrP - Cu_2^{2+}]}{[PrP - Cu^{2+}][Cu^{2+}]} \tag{4}$$

Other Cu^{2+}-binding models, such as one set of sites, two sets of sites, or sequential binding with one site, failed to converge or returned unrealistic values (e.g., exceedingly low N values). Although ITC measures the total heat change associated with a process, it should be noted that the binding-constant expressions above (eqs 1−4) do not take into account the metal−buffer interactions. Equation 5 accounts for the ACES−Cu^{2+} species that are significant at pH 7.4 and allows for the buffer-independent binding constants to be obtained from the ITC data.[26,30] The concentration of ACES buffer used in this study (10 mM) ensures that more than 98% of Cu^{2+} in solution will be in a 1:2 $Cu^{2+}/ACES$ complex. It should be noted that a set of $Cu^{2+}(ACES)_2$ complexes exist in solution that differ in the protonation state of ACES. These are described as MB_2, $M(H_{-1}B)B$, and $M(H_{-2}B)_2$, where B is the deprotonated form of ACES, H is the proton concentration, and M is the metal (eqs 6−9). At pH 7.4, the majority of Cu^{2+} exists as the $M(H_{-2}B)_2$ complex.[31,32]

$$K_{M-peptide} = K_{ITC}\left(1 + K_{MB}[B] + K_{MB_2}[B]^2 \right.$$
$$\left. + \frac{K_{MB_2}[B]^2}{K_{M(H_{-1}B)B}[H]} + \frac{K_{MB_2}[B]^2}{K_{M(H_{-1}B)_2}[H]^2}\right) \tag{5}$$

$$K_{MB} = \frac{[MB]}{[M][B]}; \quad \log K = 4.32 \tag{6}$$

$$K_{MB_2} = \frac{[MB_2]}{[M][B]^2}; \quad \log \beta = 7.77 \tag{7}$$

$$K_{M(H_{-1}B)B} = \frac{[MB_2]}{[H][M(H_{-1}B)B]}; \quad \log K = 7.36 \tag{8}$$

$$K_{M(H_{-1}B)_2} = \frac{[MB_2]}{[H]^2[M(H_{-1}B)_2]}; \quad \log \beta = 15.85 \tag{9}$$

$$K_{M-peptide} = \frac{[M - peptide]}{[M][peptide]} \tag{10}$$

The log K and log β values were obtained from ref 31 and can also be found in NIST Database 46.[31,33] Solving eq 5 yields the buffer-independent binding constants shown in Table 3. A more recent and very thorough study of Cu^{2+} complex formation by ACES is available, reporting log K and log β values different than those used in eqs 6−9.[32] Using these values to calculate the buffer-independent dissociation constants (K_d) for the first two Cu^{2+}-loading events to PrP(23−28, 57−98) yields the following values: $K_{d1} = 2$ nM, $K_{d2} = 210$ nM. These values are 2 to 3 times smaller than the calculated using values from ref 31. Thus, the values in Table 3 should be considered the upper limits for the dissociation constants.

It should be noted that there is a deviation in the fit of the ITC binding isotherm (Figure 3) at the early points in the titration (i.e., PrP/Cu^{2+} stoichiometries < 1:1). This is most likely due to the binding model used rather than the existence of ternary complexes. Although the data is consistent with the binding of two Cu^{2+} ions by the PrP(23−28, 57−98) peptide and the process can be described as two sequential binding events, the binding process is complex. Previous studies show that the 1:1 PrP/Cu^{2+} complex exists as a set of isomers involving Cu^{2+} coordination by multiple histidine residues.[15−18] Furthermore, His96 is involved as a dominant Cu^{2+}-binding ligand in the 1:1 PrP/Cu^{2+} complex and transitions to become the sole His ligand in the GTH−Cu^{2+} complex (i.e., the second Cu^{2+} bound).[18,20] Thus, the binding constants and thermodynamic values reported should be considered composite values for sets of related isomers with defined PrP/Cu^{2+} stoichiometries.

■ DISCUSSION

The use of ACES buffer, which chelates Cu^{2+}, appears to have prohibited the loading of the individual octarepeat units, a conclusion that is based on the CD spectra and fitting of the ITC data. Because an individual octarepeat unit is reported to have a mean $K_d = 7.2$ μM (log $K = 5.14$) for binding of Cu^{2+}, it is a weaker binder to Cu^{2+} by orders of magnitude (cf eqs 8 and 9).[24,31,32] Additionally, the buffer was used in a high concentration (10 mM ACES vs 0.10 mM peptide), further decreasing the ability of an octarepeat to bind Cu^{2+}. It should be noted that the isotherm in Figure 3 does not completely return to
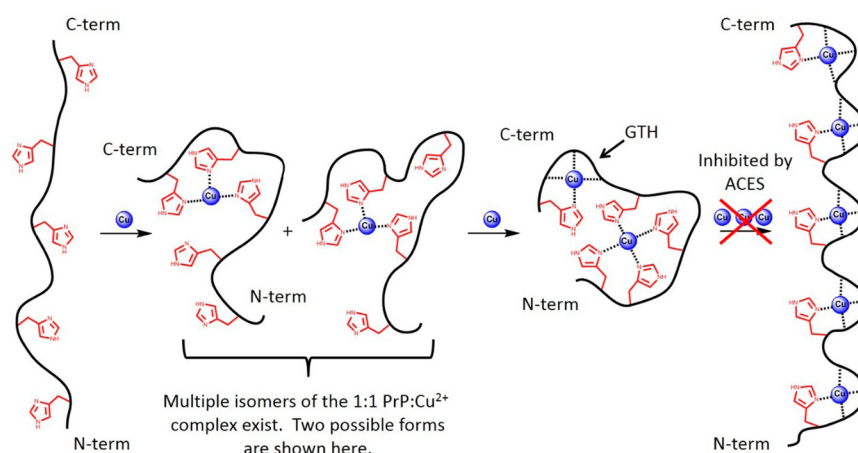
Figure 4. Illustration of Cu^{2+} loading on PrP(23−28, 57−98). Note that the last step is inhibited by the individual octarepeat sites being out-competed for Cu^+ by the ACES buffer.

baseline (i.e., 0 kcal/mol of injectant), indicating that the system is not fully saturated by Cu^{2+}. This is most likely due to the second binding site not being fully saturated at this point in the titration. It is unlikely that the octarepeats are binding to an appreciable extent because their characteristic CD signal is absent when recorded under similar conditions. Hence, the strategy of using ACES allowed for the effective isolation of the first two binding events and simplified the fitting of the ITC data.

The CD titration of PrP(23−28, 57−98) with Cu^{2+} in ACES is congruous with the loading observed in other studies: a CD silent species, attributed to coordination of Cu^{2+} by multiple His residues, forms first, followed by the binding site that is centered on His96 and composed of the residues GTH. Figure 4 shows an illustration of the PrP−Cu^{2+} species formed at different Cu^{2+} loading levels; however, the last loading step was inhibited by ACES in this study.

The use of ACES as both a buffer and a competitive ligand is well suited to this particular study because it has been well characterized; the set of complex ACES/Cu^{2+} stoichiometries and binding constants are reported.[31,32] However, applying ACES to other systems and techniques must be done with care. Besides keeping Cu^{2+} soluble under nonacidic conditions (pH > 5) where it would otherwise precipitate as a hydroxide complex, ACES brings the apparent binding affinity into a range accessible by the ITC technique. For practical purposes, the upper limit of the binding affinity reliably determined by ITC is approximately $1 \times 10^7 \text{ M}^{-1}$ ($K_d \approx 100$ nM).[30] Because a large number of protein systems have binding affinities that exceed this threshold, especially those implicated in neurodegenerative diseases,[34] ACES is a practical choice as a buffer and a competitive ligand for metal-binding studies of biomolecules.

The buffer-independent binding constants obtained from ITC are comparable to those reported by Wells et al. The dissociation constant of the first binding event is larger by a factor of 2 than that reported by Wells et al., and that of the second event is larger by a factor of 4 than that reported by Wells et al. (Table 3).[17] It is not surprising that some discrepancy exists among the K_d values determined herein and those reported by Wells et al. because two different peptide constructs were used in the study by Wells et al. (i.e., 57−91 and 91−115) to represent the different Cu^{2+}-coordination sites, whereas a single peptide encompassing the histidine-centered Cu^{2+}-binding sites was used in this study (i.e., PrP(23−28, 57−98)). Furthermore, the peptide construct consisting of residues 91−115 contains two His residues, one

Table 3. Buffer-Independent Dissociation Constants (K_d) for the First Two Cu^{2+}-Binding Events to the PrP(23−28, 57−98) Peptide

binding event	this study K_d (nM)[a]	reference 17 K_d (nM)[b]	reference 24 K_d (nM)[c]
first	7	3	0.10
second	380	100	

[a]Equation 5 was used for the calculation of the K_d values for this study. [b]Equilibrium dialysis at pH 7.4 in 5 mM TRIS buffer, constructs PrP(57−91) and PrP(91−115). [c]Fluorescence at pH 7.4 in 25 mM NEM buffer, construct PrP(23−28, 57−91).

at position 96 and the other at 111, and both appear to be capable of involvement in Cu^{2+} binding because the Cu^{2+}/peptide stoichiometry depended on the solution conditions.[14,35−37] Because the PrP peptide used here lacks His111, we are unable to comment on its role in the Cu^{2+}-binding process. The binding constant for the octarepeat domain, represented by PrP(23−28, 57−91), has also been measured by Walter et al. using fluorescence and was found to be 0.10 nM.[24] This value is over 1 order of magnitude smaller than that determined by ITC (Table 3).

Although the thermodynamic values obtained from the ITC fit parameters show that both binding events are enthalpically favorable (i.e., negative), the ΔH of the second binding event is significantly more negative. Interestingly, for the first binding event the entropy is favorable (i.e., positive) and compensates for the lower ΔH associated with it, resulting in a binding constant 2 orders of magnitude stronger than that of the second binding event. These findings may be rationalized in terms of the types of Cu^{2+}-coordination spheres associated with the two binding events. The first binding event involves the coordination of Cu^{2+} by three or four nitrogen atoms from the His imidazole rings, which are all neutral and spread throughout the flexible 57−98 region. The second binding event involves coordination by the nitrogen of a single His imidazole ring plus two or three deprotonated amide nitrogens, the latter of which are negatively charged, and all coordinating residues are adjacent to each other. Based on simple electrostatics, the negatively charged nitrogens are expected to form stronger bonds with the positively charged copper ion, resulting in a binding event with a more negative enthalpy. In terms of entropy, the first binding event involves multiple isomers of the 1:1 PrP/Cu^{2+} complex. Regardless of the

conformation in which apo-PrP exists before binding, it should be readily able to coordinate a Cu^{2+} ion without needing significant energy to reorganize. The second binding event involves the formation of a coordination sphere containing three rings (a mix of five- and six-membered rings), which must require more preorganization and/or must be more conformationally restricted.

Parallels between PrP and the amyloid beta ($A\beta$) peptide are worthy of comment because both contain sizable unstructured regions and both coordinate Cu^{2+} with high affinity.[38−40] Just like PrP, the coordination of Cu^{2+} by $A\beta$ involves an equilibrium between coordination spheres; in the case of $A\beta$, three different coordination spheres each utilize one or two His residues.[18,41] Interestingly, the thermodynamic values associated with Cu^{2+} binding by $A\beta$, as represented by peptides $A\beta16$ or $A\beta28$, mirror those of PrP: a negative ΔH and a positive $T\Delta S$.[26] In fact, the values from both studies are very close in magnitude ($A\beta16$ ΔH = −2.7 kcal/mol, $T\Delta S$ = +4.2 kcal/mol). As thermodynamic values are buffer-dependent, it should be noted that both the PrP study herein and the referenced $A\beta$ study both used ACES. Thus, a favorable entropy associated with initial metal binding may be a general property of highly flexible systems where equilibria between coordination spheres exists and multiple histidine residues are present.

CONCLUSIONS

The CD spectra and ITC data strongly suggest that PrP(23−28, 57−98) binds 2 equiv of Cu^{2+} when ACES is used as the buffer, thus preventing the individual octarepeats from taking up Cu^{2+}. The use of ACES allowed for the isolation of the first two binding events and simplified the fitting of the ITC data. The K_d values determined by ITC, 7 and 380 nM, are well in line with those reported by others. The first binding event has a considerably smaller enthalpy than the second binding event (ΔH_1 = −3.59 ± 13% kcal/mol, ΔH_2 = −37.2 ± 5% kcal/mol). However, the entropy for the first binding event is positive, whereas that of the second is significantly negative ($T\Delta S_1$ = +2.18 ± 23% kcal/mol, $T\Delta S_2$ = −34.3 ± 55% kcal/mol), offsetting the enthalpy difference leading to a K_d for the first binding event that is 2 orders of magnitude smaller (i.e., having a higher affinity). Given the similarity of the thermodynamic values associated with Cu^{2+} binding by the $A\beta$ peptide to those reported herein for PrP, a favorable entropy associated with initial metal binding (i.e., the first binding event) may be a general property of highly flexible systems containing multiple histidine residues.

ASSOCIATED CONTENT

ⓢ Supporting Information

Plots of the three individual ITC binding isotherms and a table of the thermodynamic parameters determined from each theoretical fit. This material is available free of charge via the Internet at http://pubs.acs.org.

AUTHOR INFORMATION

Corresponding Author

*E-mail: burnsc@ecu.edu.

Author Contributions

The manuscript was written through the contributions of all of the authors. All of the authors have given approval to the final version of the manuscript.

REFERENCES

(1) Stahl, N.; Borchelt, D. R.; Hsiao, K.; Prusiner, S. B. *Cell* **1987**, *51*, 229−240.

(2) Shyng, S.; Huber, M. T.; Harris, D. A. *J. Biol. Chem.* **1993**, *268*, 15922−15928.

(3) Pauly, P. C.; Harris, D. A. *J. Biol. Chem.* **1998**, *273*, 33107−33110.

(4) Brown, D. R.; Qin, K.; Herms, J. W.; Madlung, A.; Manson, J.; Strome, R.; Fraser, P. E.; Kruck, T.; von Bohlen, A.; Schulz-Schaeffer, W.; Giese, A.; Westaway, D.; Kretzschmar, H. *Nature* **1997**, *390*, 684−687.

(5) Wopfner, F.; Weidenhofer, G.; Schneider, R.; von Brunn, A.; Gilch, S.; Schwarz, T. F.; Werner, T.; Schatzl, H. M. *J. Mol. Biol.* **1999**, *289*, 1163−1178.

(6) Burns, C. S.; Aronoff-Spencer, E.; Legname, G.; Prusiner, S. B.; Antholine, W. E.; Gerfen, G. J.; Peisach, J.; Millhauser, G. L. *Biochemistry* **2003**, *42*, 6794−6803.

(7) Whittal, R. M.; Ball, H. L.; Cohen, F. E.; Burlingame, A. L.; Prusiner, S. B.; Baldwin, M. A. *Protein Sci.* **2000**, *9*, 332−343.

(8) Davies, P.; Marken, F.; Salter, S.; Brown, D. R. *Biochemistry* **2009**, *48*, 2610−2619.

(9) Kramer, M. L.; Kratzin, H. D.; Schmidt, B.; Romer, A.; Windl, O.; Liemann, S.; Hornemann, S.; Kretzschmar, H. *J. Biol. Chem.* **2001**, *276*, 16711−16719.

(10) Viles, J. H.; Cohen, F. E.; Prusiner, S. B.; Goodin, D. B.; Wright, P. E.; Dyson, H. J. *Proc. Natl. Acad. Sci. U.S.A.* **1999**, *96*, 2042−2047.

(11) Aronoff-Spencer, E.; Burns, C. S.; Avdievich, N. I.; Gerfen, G. J.; Peisach, J.; Antholine, W. E.; Ball, H. L.; Cohen, F. E.; Prusiner, S. B.; Millhauser, G. L. *Biochemistry* **2000**, *39*, 13760−13771.

(12) Burns, C. S.; Aronoff-Spencer, E.; Dunham, C. M.; Lario, P.; Avdievich, N. I.; Antholine, W. E.; Olmstead, M. M.; Vrielink, A.; Gerfen, G. J.; Peisach, J.; Scott, W. G.; Millhauser, G. L. *Biochemistry* **2002**, *41*, 3991−4001.

(13) Jackson, G. S.; Murray, I.; Laszlo, L. L. P.; Hosszu, L. P.; Gibbs, N.; Waltho, J. P.; Clarke, A. R.; Collinge, J. *Proc. Natl. Acad. Sci. U.S.A.* **2001**, *98*, 8531−8535.

(14) Jones, C. E.; Abdelraheim, S. R.; Brown, D. R.; Viles, J. H. *J. Biol. Chem.* **2004**, *279*, 32018−32027.

(15) Wells, M. A.; Jackson, G. S.; Jones, S.; Hosszu, L. P.; Craven, C. J.; Clarke, A. R.; Collinge, J.; Waltho, J. P. *Biochem. J.* **2006**, *339*, 435−444.

(16) Chattopadhyay, M.; Walter, E. D.; Newell, D. J.; Jackson, P. J.; Aronoff-Spencer, E.; Peisach, J.; Gerfen, G. J.; Bennett, B.; Antholine, W. E.; Millhauser, G. L. *J. Am. Chem. Soc.* **2005**, *127*, 12647−12656.

(17) Wells, M. A.; Jelinska, C.; Hosszu, L. P.; Craven, C. J.; Clarke, A. R.; Collinge, J.; Waltho, J. P.; Jackson, G. S. *Biochem. J.* **2006**, *400*, 501−510.

(18) Srikanth, R.; Wilson, J.; Burns, C. S.; Vachet, R. W. *Biochemistry* **2008**, *47*, 9258−9268.

(19) Davies, P.; McHugh, P. C.; Hammond, V. J.; Marken, F.; Brown, D. R. *Biochemistry* **2011**, *50*, 10781−10791.

(20) Pollock, J. B.; Cutler, P. J.; Kenney, J. M.; Gemperline, P. J.; Burns, C. S. *Anal. Biochem.* **2008**, *377*, 223−233.

(21) Hartter, D. E.; Barnea, A. *Synapse* **1988**, *2*, 412−415.

(22) Hartter, D. E.; Barnea, A. *J. Biol. Chem.* **1988**, *263*, 799−805.

(23) Hopt, A.; Korte, S.; Fink, H.; Panne, U.; Niessner, R.; Jahn, R.; Kretzschmar, H.; Herms, J. *J. Neurosci. Methods* **2003**, *128*, 159−172.

(24) Walter, E. D.; Chattopadhyay, M.; Millhauser, G. L. *Biochemistry* **2006**, *45*, 13083−13092.

(25) Thompsett, A. R.; Abdelraheim, S. R.; Daniels, M.; Brown, D. R. *J. Biol. Chem.* **2005**, *280*, 42750−42758.

(26) Sacco, C.; Skowronsky, R. A.; Gade, S.; Kenney, J. M.; Spuches, A. M. *J. Biol. Inorg. Chem.* **2012**, *17*, 531−541.

(27) Klewpatinond, M.; Viles, J. H. *FEBS Lett.* **2007**, *581*, 1430−1434.

(28) Garnett, A. P.; Viles, J. H. *J. Biol. Chem.* **2003**, *278*, 6795−6802.

(29) Klewpatinond, M.; Davies, P.; Bowen, S.; Brown, D. R.; Viles, J. H. *J. Biol. Chem.* **2008**, *283*, 1870−1881.

(30) Grossoehme, N. E.; Spuches, A. M.; Wilcox, D. E. *J. Biol. Inorg. Chem.* **2010**, *15*, 1183−1191.

(31) Pope, J. M.; Stevens, P. R.; Angotti, M. T.; Nakon, R. *Anal. Biochem.* **1980**, *103*, 214−221.

(32) Zawisza, I.; Rogza, M.; Poznanski, J.; Bal, W. *J. Inorg. Biochem.* **2013**, *129*, 58−61.

(33) *NIST Standard Reference Database 46. NIST Critically Selected Stability Constants of Metal Complexes Database*, version 8.0; Martell, A. E., Smith, R. M., Eds.; National Institute of Standards and Technology: Gaithersburg, MD, 2004. http://www.nist.gov/srd/nist46.cfm.

(34) Zawisza, I.; Rozga, M.; Bal, W. *Coord. Chem. Rev.* **2012**, *256*, 2297−2307.

(35) Klewpatinond, M.; Viles, J. H. *Biochem. J.* **2007**, *404*, 393−402.

(36) Berti, F.; Gaggelli, E.; Guerrini, R.; Janicka, A.; Kozlowski, H.; Legowska, A.; Miecznikowska, H.; Migliorini, C.; Pogni, R.; Remelli, M.; Rolka, K.; Valensin, D.; Valensin, G. *Chem.—Eur. J.* **2007**, *13*, 1991−2001.

(37) Rivillas-Acevedo, L.; Grande-Aztatzi, R.; Lomelı, I.; Garcia, J. E.; Barrios, E.; Teloxa, S.; Vela, A.; Quintanar, L. *Inorg. Chem.* **2011**, *50*, 1956−1972.

(38) Sgourakis, N. G.; Yan, Y.; McCallum, S. A.; Wang, C.; Garcia, A. E. *J. Mol. Biol.* **2007**, *368*, 1448−1457.

(39) Vivekanandan, S.; Brender, J. R.; Lee, S. Y.; Ramamoorthy, A. *Biochem. Biophys. Res. Commun.* **2011**, *411*, 312−316.

(40) Faller, P.; Hureau, C. *Dalton Trans.* **2009**, 1080−1094.

(41) Hong, L.; Carducci, T. M.; Bush, W. D.; Dudzik, C. G.; Millhauser, G. L.; Simon, J. D. *J. Phys. Chem. B* **2010**, *114*, 11261−11271.